

## Grid multi-wing butterfly chaotic attractors generated from a new 3-D quadratic autonomous system

Xiaowen Luo, Chunhua Wang, Zhao Wan

College of Information Science and Engineering, Hunan University  
Changsha 410082, China  
wch1227164@sina.com

**Received:** 20 November 2012 / **Revised:** 25 August 2013 / **Published online:** 19 February 2014

**Abstract.** Due to the dynamic characteristics of the Lorenz system, multi-wing chaotic systems are still confined in the positive half-space and fail to break the threshold limit. In this paper, a new approach for generating complex grid multi-wing attractors that can break the threshold limit via a novel nonlinear modulating function is proposed from the firstly proposed double-wing chaotic system. The proposed method is different from that of classical multi-scroll chaotic attractors generated by odd-symmetric multi-segment linear functions from Chua system. The new system is autonomous and can generate various grid multi-wing butterfly chaotic attractors without requiring any external forcing, it also can produce grid multi-wing both on the  $xz$ -plane and  $yz$ -plane. Basic properties of the new system such as dissipation property, equilibrium, stability, the Lyapunov exponent spectrum and bifurcation diagram are introduced by numerical simulation, theoretical analysis and circuit experiment, which confirm that the multi-wing attractors chaotic system has more rich and complicated chaotic dynamics. Finally, a novel module-based unified circuit is designed which provides some principles and guidelines for future circuitry design and engineering application. The circuit experimental results are consistent with the numerical simulation results.

**Keywords:** a new 3-D chaotic system, Lyapunov exponent, nonlinear functions, grid multi-wing butterfly attractors.

### 1 Introduction

Along with the people to deep research of the nonlinear system chaotic phenomenon and chaotic application, chaos in the electronic, communication, information processing, cranial nerve science and other areas of application has caused wide attention [1–6]. Creating a chaotic system with a more complicated topological structure such as multi-scroll or multi-wing attractors, therefore, becomes a desirable task and sometimes a key issue for many engineering applications. Now, many multi-scroll chaotic attractors have been designed and implemented over the past two decades [7–9]. Based on the Chua system, by constructing odd-symmetric multi-segment linear functions, saw tooth wave, triangle wave, step wave, hysteresis sequence and saturated sequence, multi-scroll chaotic attractors can be obtained. For example, Suykens proposed a family of  $n$ -double scroll

chaotic attractors [10]; Tang et al. introduced a sine-function approach for generating  $n$ -scroll chaotic attractors [11], with a systematical circuit realization that can physically produce up to as many as ten scrolls visible on the oscilloscope; Suykens et al. proposed a new approach for generation of  $n$ -double scrolls [12]; Lü and Chen discovered saturated function series and triangular wave series approaches, respectively, for generating multi-scroll chaotic attractors [13, 14], although the works on generating and analyzing  $n \times m$ -scroll attractors have been widely reported recently, with a comprehensive review given in [14], however, how to generate multi-wing chaotic attractors are still rarely reported, the main reason is that the limitation of the threshold effect, most of the chaotic systems are limited in positive half-space or its mirror of negative half-space. Lü et al. introduced some chaotic systems which can obtain double-wing, three-wing and four-wing chaotic attractors [15–19], famous butterfly attractor of Lorenz equation model is a paradigm in chaos and is one of the most important models in the study of chaotic dynamics, a large number of its variants, including Chen and Lü systems with generating double-wing butterfly attractors, have been proposed and studied recently under the framework of a generalized Lorenz system family, several four-wing chaotic attractors have been obtained from the Liu system [20] and augmented Lü system [21] as well as various of their modified models, but their methods mainly depend on system simulation findings and their works don't form a concert method, the numbers of chaotic attractors are also very limited. Zhang et al. introduced several methods for generating multi-wing chaotic system but still failed to break the threshold limit [22], the wings of the attractors are only extended in single direction, so they can not generate more complex grid multi-wing chaotic systems. Yu proposed an approach generation of unidirectional  $n \times m$ -wing Lorenz-like attractors from a modified Shimizu–Morioka model [23], in 2011, Yu et al. realized the generalized grid multi-wing chaotic attractors by constructing heteroclinic loops into switching systems [24], but the system is complex and hard for circuit implementation, it has no practical application. In 2012, Yu et al. constructed grid multi-wing hyperchaotic Lorenz system family via switching control and constructing super-heteroclinic loops [25], but it only generates grid multi-wing on the  $xz$ -plane and is also complex for circuit implementation. So finding and designing a new and simple grid multi-wing chaotic system that can break the threshold limit and generate multi-wing chaotic attractors especially grid multi-wing chaotic attractors on the multi-plane is still a challenging and important hotspot.

To break the threshold limit with respect to the vertical axis, this paper firstly proposes a new three dimensional and quadratic modified Lorenz system, which can produce a typical double-wing butterfly chaotic attractors. According to the double-wing character of chaotic system, we design a parameter adjustable piecewise square function and a new stair function combining with sign function, so that the saddle-focus points of the system of index 2 are extended in the fixed  $y$  and  $z$  direction which can break the threshold limit. This new system introduced in Section 2 is autonomous and easy for circuit implementation, and yet, it can produce complex grid multi-wing attractors both on the  $xz$ -plane and  $yz$ -plane which is different from the systems [26–28]. Since it possesses a similar adaptive feature, outperforming those Chua-circuit-based multi-scroll systems, while at the same time, it exhibits more complicated chaotic dynamics than its double-wing or

four-wing,  $n$ -wing counterpart chaotic systems. Moreover, the proposed model provides additional design flexibility for richer chaotic dynamics, allowing arbitrary selection of the numbers of wings both on the  $xz$ -plane and  $yz$ -plane and their locations, giving a wider range of parametric choices. Analysis of the basic dynamics of grid multi-wing chaotic system, including symmetry and dissipation characteristic, the distribution of equilibrium points, Poincaré maps, the time domain waveform, spectrum, bifurcation diagram and the maximum Lyapunov exponent spectrum are also given in Section 3. In order to confirm the effectiveness of the proposed method, an oscillator circuit is designed for implementation and the circuit experimental results are consistent with the numerical simulation results which are demonstrated in Section 4, so it is easy for circuit implementation and has wide applications in various fields such as the genetic networks and hybrid image encryption. Finally, a conclusion is given in Section 5.

## 2 Design of grid multi-wing butterfly attractors chaotic system

This section discusses the design of grid multi-wing chaotic system, firstly we propose a new 3-D quadratic autonomous generalized Lorenz system which can produce a typical double-wing chaotic attractors, and then through designing the corresponding nonlinear functions, it can be expanded into  $(2N + 2) \times (2M + 2)$  multi-wing attractors chaotic system.

### 2.1 A new 3-D quadratic autonomous generalized Lorenz system

Considering a new 3-D quadratic autonomous generalized Lorenz system which can produce double-wing chaotic attractors, the proposed new dimensionless system is as follows:

$$\frac{dx}{dt} = a(y - x), \quad \frac{dy}{dt} = by - zx, \quad \frac{dz}{dt} = g(y) - c. \quad (1)$$

Here  $a, b, c \in \mathbb{R}^+$ , which are state variables, and  $g(y) = y^2$ . When  $a = 2$ ,  $b = 0.6$ ,  $c = 0.49$ , numerical simulation results of the double-wing chaotic attractors are depicted in Fig. 1. The equilibrium points of (1) can be easily derived:  $Q_0(0, 0, 0)$ ,  $Q_1(0.7, 0.7, 0.6)$

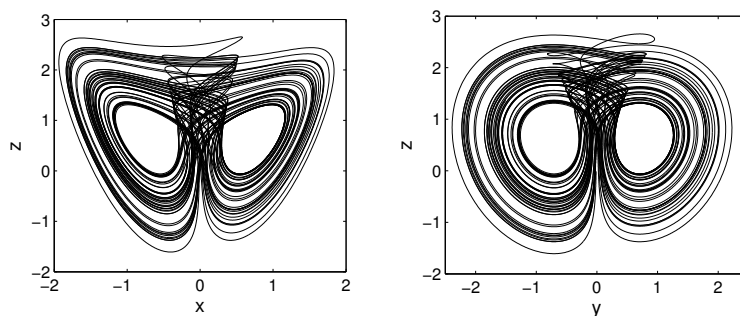


Fig. 1. Double-wing butterfly chaotic attractors of the system (1) on the  $xz$ -plane,  $yz$ -plane.

and  $Q_2(-0.7, -0.7, 0.6)$ , equilibrium points can be used to calculate the eigenvalues which are following:  $\lambda_1 = -2, \lambda_2 = 0.6$  and  $\lambda_3 = 0$ . For  $Q_1$  and  $Q_2$ , they have the same eigenvalues:  $\lambda_1 = -1.5706, \lambda_2 = 0.0853 + 1.1138i$  and  $\lambda_3 = 0.0853 - 1.1138i$ , where there is a negative eigenvalue and the other two are conjugate complex numbers of which the real parts are positive, so they are the unstable saddle-focus points of index 2. Through the literature [28], we know that the double-wing chaotic attractors develop from the unstable saddle-focus points of index 2:  $Q_1$  and  $Q_2$ . Three Lyapunov exponents of the new 3-D chaotic system are:  $\lambda_{L1} = 0.1322, \lambda_{L2} = 0.0000$  and  $\lambda_{L3} = -0.6178$ , respectively, where it has a positive Lyapunov exponent, confirming system (1) chaotic characteristic.

**2.2 A new 3-D quadratic autonomous generalized Lorenz system**

Chaotic system (1) the same as most generalized Lorenz system, can produce a double-wing chaotic attractors around the two unstable saddle-focus points, but the chaotic dynamics of system (1) are confined to the positive half-space with respect to the  $z$ -axis, so multi-wing (multi-scroll) chaotic system design criterion is that designing suitable nonlinear functions to expand saddle-focus points of index 2 of the system on the plane or in the space. Based on the thought of breaking threshold effect, we will transform  $g(y)$  of system (1) into a parameter adjustable multi-piecewise square function defined by  $f_N(y)$ , which is described in system (2) and also can make the wings of system extended in the  $x$  and  $y$  direction obviously. The numerical simulation results of plane phase diagram are shown in Fig. 2.

$$\frac{dx}{dt} = a(y - x), \quad \frac{dy}{dt} = by - zx, \quad \frac{dz}{dt} = f_N(y) - c, \quad (2)$$

where  $f_N(y) = g(y) + \sum_{i=1}^N \{A_i[\text{sgn}(y + a_i) - \text{sgn}(y - a_i) - 2]\}$ ,  $a_i$  use the same values, and  $\sum_{i=1}^N A_i = iK(i + 1.2)$ , here  $K = 0.5$ . The adjustable parameters:  $A_i, a_i$  are described in Table 1.

Also the design of a new stair function defined by  $f_M(z)$  and the  $\text{sgn}$  function defined by  $\text{sgn}(z)$  can realize the extension of wings in the  $z$  direction. So a new complex grid

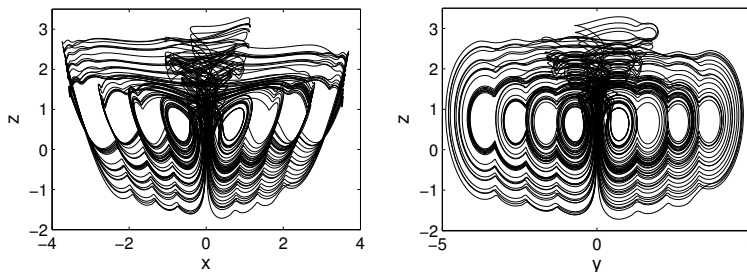


Fig. 2. Multi-wing attractors on the  $xz$ -plane,  $yz$ -plane: 8-wing.

Table 1. Values of adjustable parameters  $A_i, a_i$ .

$N$	$A_1$	$A_2$	$A_3$	$a_1$	$a_2$	$a_3$
1	1.1			1.3		
2	1.1	2.1		1.3	2.3	
3	1.1	2.1	3.1	1.3	2.3	3.3

Table 2. Values of adjustable parameters  $B_j, b_j$ .

$M$	$B_1$	$B_2$	$b_1$	$b_2$
1	1.1		3	
2	1.1	1.1	3	5

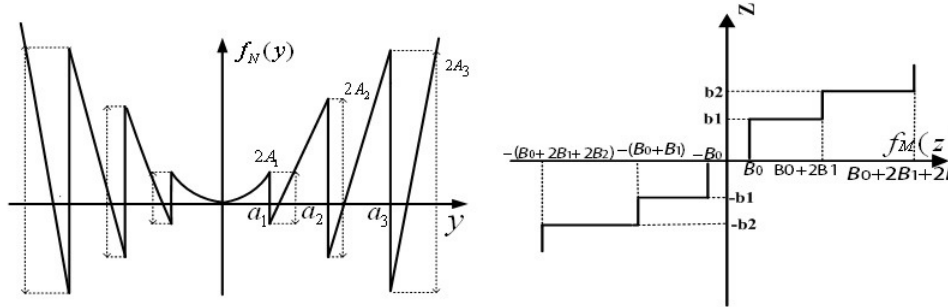


Fig. 3. The nonlinear functions: the parameter adjustable multi-piecewise square function  $f_N(y)$  (left), the new stair function  $f_M(z)$  (right).

multi-wing chaotic system model is described as

$$\begin{aligned}
 \frac{dx}{dt} &= a(y - x), \\
 \frac{dy}{dt} &= by - \text{sgn}(z)x(z - f_M(z)), \\
 \frac{dz}{dt} &= [f_N(y) - c] \text{sgn}(z),
 \end{aligned}
 \tag{3}$$

where

$$\text{sgn}(z) = \begin{cases} -1, & z < 0, \\ 0, & z = 0, \\ 1, & z > 0. \end{cases}
 \tag{4}$$

$f_M(z) = B_0 \text{sgn}(z) + \sum_{j=1}^M \{B_j [\text{sgn}(z + b_j) + \text{sgn}(z - b_j)]\}$ ,  $0 \leq i \leq N$ ,  $0 \leq j \leq M$ ,  $M, N = 0, 1, 2, \dots$ , and  $A_i, a_i, B_j, b_j$  are all adjustable parameters.  $N, M$  are the numbers of accumulation item, the nonlinear functions:  $f_N(y)$  and  $f_M(z)$  are shown in Fig. 3 respectively. In order to make the chaotic attractors uniformly distributed in space, the adjustable parameters meet the relations which are following:  $B_0 = B_j = 1.1$ ,  $b_j = 2j + 1$ ,  $0 \leq j \leq M$ . It is easy to calculate the values of adjustable parameters:  $B_j, b_j$ , which are shown in Table 2.

According to type (3) and Tables 1, 2, it can exhibit grid multi-wing chaotic attractors, the numbers of grid multi-wing attractors depend on the concrete form of  $f_N(y)$  and  $f_M(z)$  and the values of adjustable parameters:  $A_i, a_i, B_i, b_i$ , which play a key role for breaking the threshold limit above and generating various multi-wing butterfly chaotic attractors. For example, when  $N = 2, M = 1$ , it can exhibit  $6 \times 4$ -wing chaotic attractors

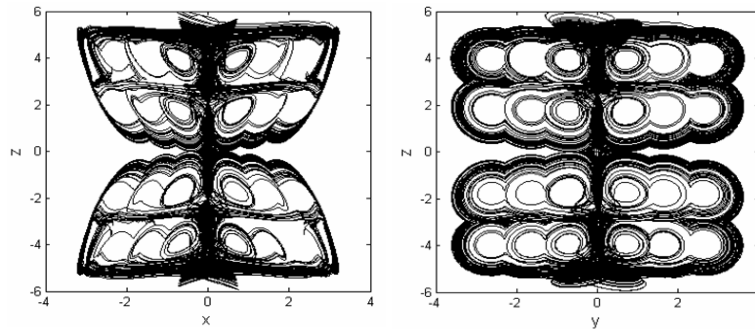


Fig. 4.  $6 \times 4$ -wing chaotic attractors on the  $xz$ -plane,  $yz$ -plane.

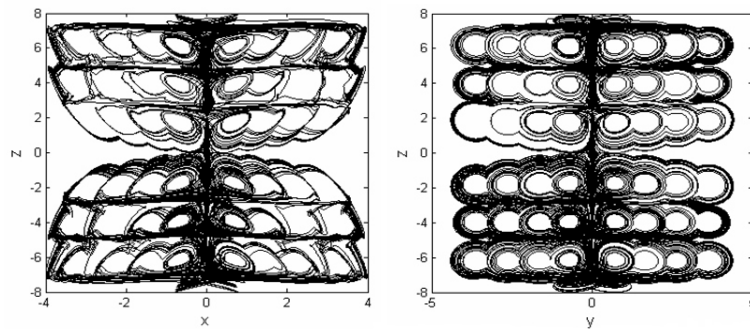


Fig. 5.  $8 \times 6$ -wing chaotic attractors on the  $xz$ -plane,  $yz$ -plane.

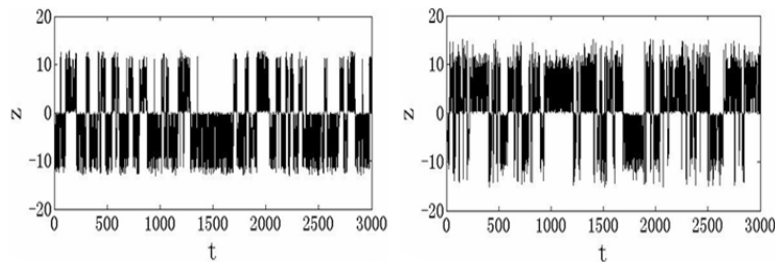


Fig. 6. Time domain waveforms  $z(t)$  of the grid multi-wing chaotic attractors:  $6 \times 4$ -wing (left),  $8 \times 6$ -wing (right).

which are shown in Fig. 4, when  $N = 3$ ,  $M = 2$ , it can exhibit  $8 \times 6$ -wing chaotic attractors which are shown in Fig. 5, where it shows a few more complex grid multi-wing attractors phase diagram. Figure 6 shows the time domain waveforms of some kinds of grid multi-wing attractors, when phase trajectory enters from one region into another region, it can return back to the original region due to the role of unstable equilibrium points. It obviously shows that the system attractors can come through back and forth freely in the positive half-space and negative half-space.

### 3 Basic dynamics analysis

This section has analyzed basic dynamic characteristics of the grid multi-wing chaotic system (3), including dissipation characteristic, equilibrium point distribution of the system, system analysis in the time domain and frequency domain, the bifurcation diagram, the maximum Lyapunov exponent spectrum analysis with the change of parameter  $a$ .

#### 3.1 Symmetry and dissipation characteristic

For variable substitution of the system:  $(x, y, z) \rightarrow (-x, -y, -z)$ , its type form is still the same, it is easy to know that system (3) is symmetrical about original point. Since

$$\nabla V = \frac{\partial f_1}{\partial x} + \frac{\partial f_2}{\partial y} + \frac{\partial f_3}{\partial z} = -2 + 0.6 = -1.4 < 0. \quad (5)$$

System (3) is dissipative, and due to the index form:  $dV/dt = e^{-1.4t}$ , it converges to volume element  $V_0$  in time  $t$ , so its form of convergence for volume element is  $V_0 e^{-1.4t}$ , which means that all system trajectory will be limited to the point of zero volume set, its behavior will be fixed in the attractor when  $t \rightarrow \infty$ .

#### 3.2 Equilibrium point distribution and its stability

According to type (3), setting  $dx/dt = dy/dt = dz/dt = 0$ , equilibrium point equation is following:

$$\begin{aligned} 2(y - x) &= 0, \\ 0.6y - x \operatorname{sgn}(z)(z - f_M(z)) &= 0, \\ [f_N(y) - 0.49] \operatorname{sgn}(z) &= 0. \end{aligned} \quad (6)$$

In addition to equilibrium point  $Q(0, 0, 0)$ , through type (6), the rest equilibrium points  $Q(x_{\pm n}^{(q)}, y_{\pm n}^{(q)}, z_{\pm m}^{(q)})$  are described as follows:

$$\begin{aligned} x_{\pm n}^{(q)} = y_{\pm n}^{(q)} &= \begin{cases} \pm 0.7, & n = 0, \\ \pm \sqrt{0.49 + 2 \sum_{i=1}^n A_i}, & 1 \leq n \leq N, \end{cases} \\ z_{\pm m}^{(q)} &= \begin{cases} \pm 1.7, & m = 0, \\ \pm (1.7 + 2 \sum_{j=1}^m B_j), & 1 \leq m \leq M. \end{cases} \end{aligned} \quad (7)$$

According to related values in Tables 1, 2 and type (7), setting  $N = 3$ ,  $M = 2$ , the distributions of equilibrium points on the  $yz$ -plane are shown in Fig. 7, where  $\bullet$  denotes the saddle-focus points of index 2. It is obvious observed that through introducing parameter adjustable multi-piecewise square function  $f_N(y)$ , a new stair function  $f_M(z)$ , which is different from literature [28], system (3) contains square function and can generate grid multi-wing attractors, so it has more complex dynamics characteristics, literatures only

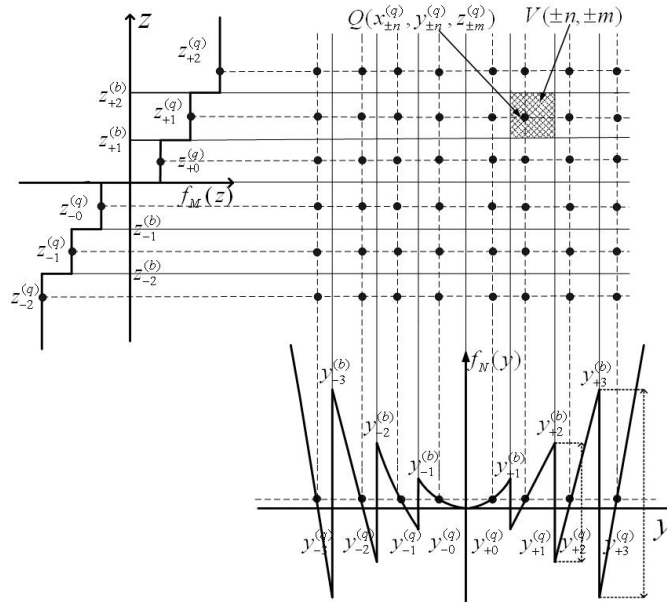


Fig. 7. Equilibrium points and boundary lines of  $8 \times 6$  grid multi-wing butterfly chaotic attractors.

can generate multi-scroll attractors by using piecewise-linear functions, cellular neural networks, nonlinear modulating functions, also the two unstable saddle-focus points of the original system (1) have been extended into  $(2N + 2) \times (2M + 2)$  unstable saddle-focus points both on  $yz$ -plane and  $xz$ -plane, so system (3) can generate grid multi-wing attractors both on  $yz$ -plane and  $xz$ -plane. The equilibrium points  $Q(x_{\pm n}^{(q)}, y_{\pm n}^{(q)}, z_{\pm m}^{(q)})$  of the  $8 \times 6$ -wing chaotic attractors are described as follows:

$$\begin{aligned}
 x_{\pm 0}^{(q)} = y_{\pm 0}^{(q)} = \pm 0.700, & \quad x_{\pm 1}^{(q)} = y_{\pm 1}^{(q)} = \pm 1.640, \\
 x_{\pm 2}^{(q)} = y_{\pm 2}^{(q)} = \pm 2.625, & \quad x_{\pm 3}^{(q)} = y_{\pm 3}^{(q)} = \pm 3.618, \\
 z_{\pm 0}^{(q)} = \pm 1.700, & \quad z_{\pm 1}^{(q)} = \pm 3.900, \quad z_{\pm 2}^{(q)} = \pm 6.100.
 \end{aligned} \tag{8}$$

By linearizing system (3), the result of Jacobin matrix at the equilibrium points  $Q(x_{\pm n}^{(q)}, y_{\pm n}^{(q)}, z_{\pm m}^{(q)})$  is given in Eq. (9).

$$J_Q = \begin{bmatrix} -2 & 2 & 0 \\ (K_1 - z_{\pm m}^{(q)}) \times K_2 & 0 & -x_{\pm n}^{(q)} \times K_2 \\ 0 & 2y_{\pm n}^{(q)} \times K_2 & 0 \end{bmatrix}. \tag{9}$$

Among them,  $K_1 = f_M(z_{\pm m}^{(q)})$ ,  $K_2 = \text{sgn}(z_{\pm m}^{(q)})$  are the corresponding values in the equilibrium points. In order to study the stability of the system, considering the corresponding Jacobian matrix of each equilibrium point and calculating the eigenvalue,

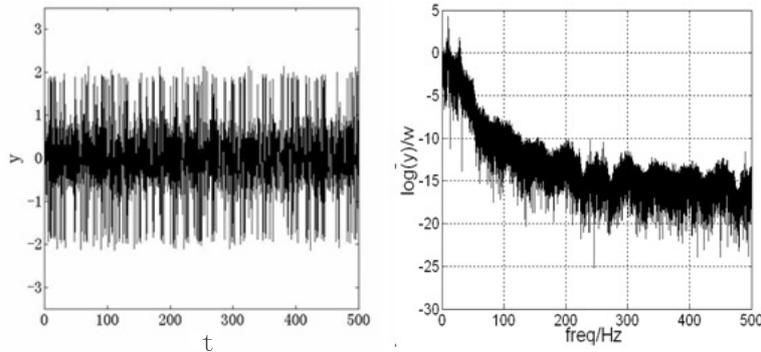


Fig. 8. Dynamic analysis: time domain waveform  $y(t)$  (left), frequency spectrum  $\log |y|$  (right).

the result shows that 48 equilibrium points are all saddle-focus equilibrium points of index 2 using  $\bullet$  described in Fig. 7, and each of them can produce a corresponding wing. Fig. 8 (left) shows the time domain waveform  $y(t)$  of system (3), combining with Fig. 3, we can see the phase track is infinite filling or wandering in a certain area, which is the typical nonperiodic. Fig. 8 (right) shows the spectrum of system (3), we can see the spectrum is continuous in certain frequency range, further shows it nonperiodic.

### 3.3 Poincaré maps, bifurcation diagram and the maximum Lyapunov exponent

The Poincaré map is an important analysis technique for understanding chaotic dynamics. Fig. 9 shows different sections for plane:  $x = 0$  and  $y = 0$ , the Poincaré maps here consist of many branches with a number of twigs, which implies that the orbits of the attractor are continuously folded and bifurcated in different directions, from periodic oscillations to chaos is clearly observed, and it indicates that the system has extremely rich dynamics.

According to type (3) and (4), bifurcation diagram and the maximum Lyapunov exponent spectrum with the changing of parameter  $a$  when  $b = 0.6$ ,  $c = 0.49$  are shown

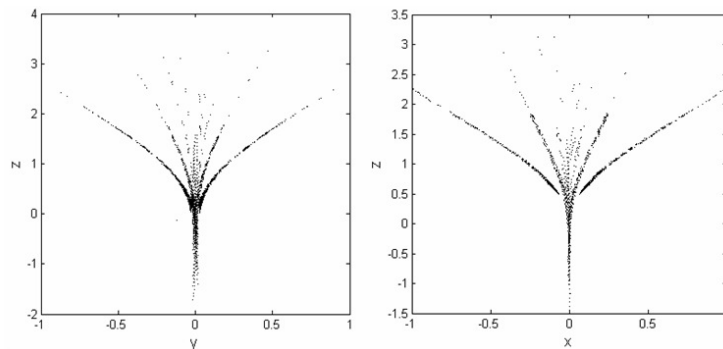


Fig. 9. Poincaré maps of system (1) when  $a = 2$ ,  $b = 0.6$ ,  $c = 0.49$  on different crossing sections:  $y = 0$  (left),  $x = 0$  (right).

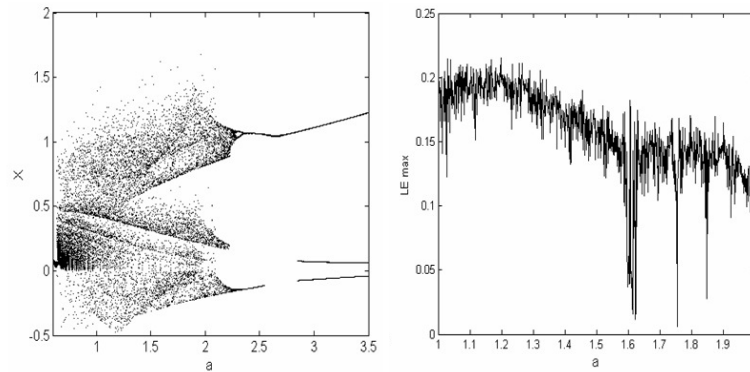


Fig. 10. Bifurcation diagram versus  $a$  (left), the maximum Lyapunov exponent spectrum versus  $a$  (right).

in Fig. 10, we can see system (3) has a positive Lyapunov exponent in a certain range, and bifurcation diagram has very good consistency with the maximum Lyapunov exponent spectrum. It is verified that the system (3) can generate different numbers of wings through different values of parameter  $a$ . Therefore, from each plane phase of system (3), the time domain waveform, spectrum, bifurcation diagram and the maximum Lyapunov exponent (LE) spectrum, which reflects bifurcation and folding properties of chaos and the extremely rich dynamics of system (3). Where the existence of positive LE implies the chaotic nature of the system.

#### 4 Circuit realization and experimental results

Based on the proposed grid multi-wing chaotic system in this paper, the integral design of the analog circuit is shown in Fig. 11. Circuit design uses the linear resistance, linear capacitance, analog multiplier and operational amplifier. The analog multiplier uses *AD633*, multiplication factor is 0.1. The op-amp in use is *TL082* with saturated voltage of  $\pm|V_{sat}| = \pm 13.5$  V, assuming the dual voltage sources of  $\pm E_{sat} = \pm 15$  V. In addition, for time scale transformation factor, or integral constant of integrator, we use time scale transformation factor:  $\tau_0 = R_0 C_0$ , which does not change the shape of phase portrait, but only increases the vibration frequency of the chaotic circuit and chaotic signal spectrum distribution range, it is very important on selecting the time scale and changing the size of the factor reasonable in the chaotic circuit design, where  $R_0 = 10$  k $\Omega$ ,  $C_0 = 33$  nF are used. Taking the multi-plane grid multi-wing chaotic attractors for an example of the design of the circuit, the subcircuit diagrams for realizing the nonlinear functions  $f_N(y)$  and  $f_M(z)$  above are respectively depicted in Fig. 12, the corresponding circuit parameters are omitted here because of the space limit. It should be emphasized that the numbers of wings can be easily modified by using different numbers of modular blocks which are shown in Fig. 12. Realization of the sign function is also given in Fig. 12 for reference. What emphasize is that through the use of the switch  $S$  control different numbers of module access as shown in Fig. 12, which can adjust the values of natural

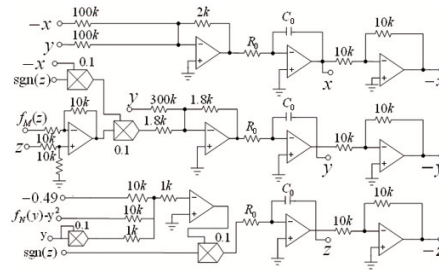


Fig. 11. Module-based circuit diagram for implementation of the grid multi-wing chaotic system.

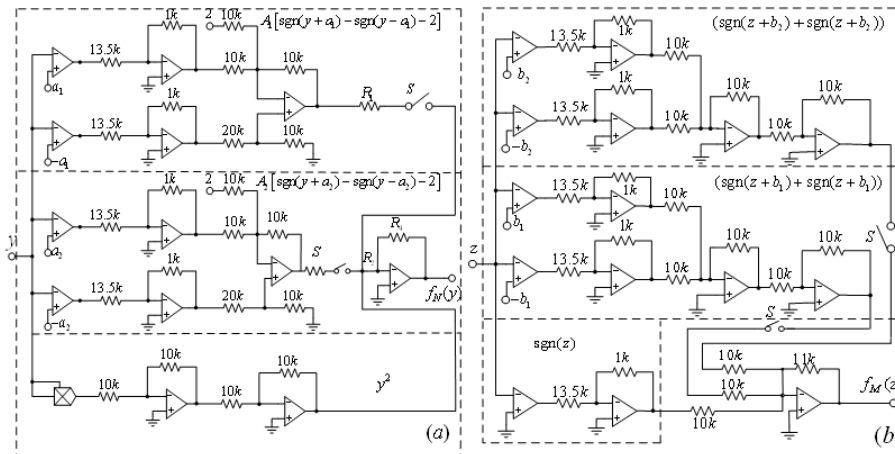


Fig. 12. The parameter adjustable multi-pieces square function  $f_N(y)$  (left), stair function  $f_M(z)$  (right).

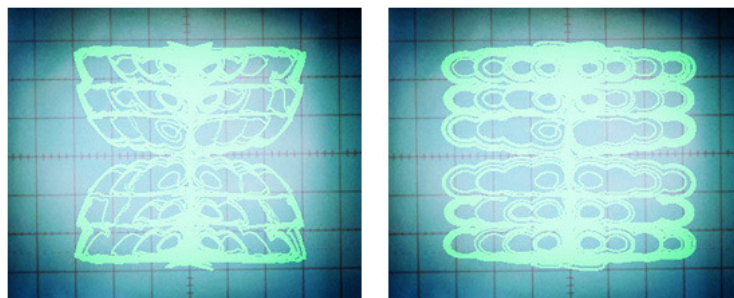


Fig. 13. Circuit experimental results of grid multi-wing chaotic attractors on the  $xz$ -plane,  $yz$ -plane:  $8 \times 6$ -wing.

numbers  $N$  and  $M$  flexibly. Figure 13 shows circuit experimental results of the grid multi-wing chaotic attractors, we can see that circuit experimental results is basically consistent with the numerical simulation result, confirming the correctness of the theoretical analysis and the feasibility of circuit design of grid multi-wing chaotic attractors.

## 5 Conclusions

This paper has proposed a novel three dimensional quadratic chaotic system which can produce a typical double-wing chaotic attractors, then we have introduced a novel Lorenz-like system which can generate complex grid multi-wing chaotic attractors through circuit designing implementations. The numerical simulations show that the system has interesting and complex dynamical behaviors. The main character of grid multi-wing system is that adjustable parameter can be flexibly adjusted for saddle-focus points of index 2 distribution in the  $y$  direction and  $z$  direction plane space, which can be convenient to control numbers, sizes and relative positions of the wings. It should be pointed out that one of the fundamental design principles for breaking the threshold is to insert nonlinear functions. Through the theory analysis and numerical simulation, we have analyzed basic dynamic characteristics of the grid multi-wing chaotic system. Finally, the analog circuit design of realizing the grid multi-wing chaotic system, the consistency of circuit experimental results and the numerical simulation results prove the feasibility of the structure method. Furthermore, multi-wing butterfly chaotic attractors have the general applications in engineering, such as the genetic networks and hybrid image encryption, random number generation, secure communication and efficient liquid mixing.

## References

1. G.L. Cai, J.J. Huang, Synchronization for hyperchaotic Chen system and hyperchaotic Rossler system with different structure, *Acta Phys. Sin.*, **55**(8):3997–4004, 2008.
2. D.M. Chen, Z.L. Zhu, G.M. Yang, An improved image encryption algorithm based on chaos, in: *Proceedings of the 9th International Conference for Young Computer Scientists (Zhang Jia Jie, Hunan, China, November 18–21, 2008)*, IEEE Computer Society, Los Alamitos, CA, Washington, Tokyo, 2008, pp. 2792–2796.
3. S. Demirkol, S. Özoğuz, V. Tavas, S. Kiliç, A CMOS realization of double-scroll chaotic circuit and its application to random number generation, in: *Proceedings of IEEE International Symposium on Circuits and Systems (Seattle, Washington, USA, May 18–21, 2008)*, IEEE, Los Alamitos, CA, 2008, pp. 2374–2377.
4. Y. Lin, C.H. Wang, H.Xu, Grid multi-scroll chaotic attractors in hybrid image encryption algorithm based on current conveyor, *Acta Phys. Sin.*, **61**(24), 240503, 9 pp., 2012.
5. H.M. Srivastava, A.K. Mishra, Applications of fractional calculus to parabolic starlike and uniformly convex functions, *Comput. Math. Appl.*, **39**(3–4):57–69, 2000.
6. P. Wang, J.H. Lü, M.J. Ogorzalek, Global relative parameter sensitivities of the feed-forward loops in genetic networks, *Neurocomputing*, **78**(1):155–165, 2012.
7. J.H. Lü, G.R. Chen, Generating multiscroll chaotic attractors: Theories, methods and applications, *Int. J. Bifurcation Chaos Appl. Sci. Eng.*, **16**(4):755–858, 2006.
8. J.H. Lü, G.R. Chen, X.H. Yu, H. Leung, Design and analysis of multi-scroll chaotic attractors from saturated function series, *IEEE Trans. Circuits Syst.*, **51**(12):2476–2490, 2004.

9. J.H. Lü, S.M. Yu, G.R. Chen, H. Leung, Experimental verification of multidirectional multiscroll chaotic attractors, *IEEE Trans. Circuits Syst., I, Fundam. Theory Appl.*, **53**(1):149–165, 2006.
10. J.A.K. Suykens, A. Huang, L.O. Chua, A family of  $n$ -scroll attractors from a generalized Chua's circuit, *Int. J. Electron.*, **51**(3):131–138, 1997.
11. W.K.S. Tang, G.Q. Zhong, G.Chen, K.F. Man, Generation of  $n$ -scroll attractors via sine function, *IEEE Trans. Circuits Syst., I, Fundam. Theory Appl.*, **48**(11):1369–1372, 2001.
12. J.A.K. Suykens, J. Vandewalle, Generation of  $n$ -double scrolls ( $n = 1, 2, 3, 4, \dots$ ), *IEEE Trans. Circuits Syst. I, Fundam. Theory Appl.*, **40**(11):861–867, 1993.
13. S.M. Yu, J.H. Lü, W.K.S. Tang, G.R. Chen, A general multiscroll Lorenz system family and its realization via digital signal processors, *Chaos*, **16**(3), 033126, 10 pp., 2006.
14. S.M. Yu, W.K.S. Tang, G.Chen, Generation of  $n \times m$ -scroll attractors under a Chua-circuit framework, *Int. J. Bifurcation Chaos Appl. Sci. Eng.*, **17**(11):3951–3964, 2007.
15. S.J. Cang, G.Y. Qi, Z.Q. Chen, A four-wing-hyper-chaotic attractor and transient chaos generated from a new 4-D quadratic autonomous system, *Nonlinear Dyn.*, **59**:515–527, 2010.
16. Z.Q. Chen, Y.Yang, Z.Z. Yuan, A single three-wing or four-wing chaotic attractor generated from a three-dimensional smooth quadratic autonomous system, *Chaos Solitons Fractals*, **38**(4):1187–1196, 2008.
17. A.S. Elwakil, S. Özoğuz, M.P. Kennedy, A four wing butterfly attractor from a fully autonomous system, *Int. J. Bifurcation Chaos Appl. Sci. Eng.*, **13**(10):3093–3098, 2003.
18. G.Y. Qi, G.R. Chen, M.A. V. Wyk, B.J.V. Wyk, Y.H. Zhang, A four-wing chaotic attractor generated from a new 3-D quadratic autonomous system, *Chaos Solitons Fractals*, **38**(3):705–721, 2008.
19. S.M. Yu, W.K.S. Tang, Tetrapterous butterfly attractors in modified Lorenz systems, *Chaos Solitons Fractals*, **41**(4):1740–1749, 2009.
20. G.R. Chen, T. Ueta, Yet another chaotic attractor, *Int. J. Bifurcation Chaos Appl. Sci. Eng.*, **9**(6):1465–1466, 1999.
21. J.H. Lü, G.R. Chen, A new chaotic attractor coined, *Int. J. Bifurcation Chaos Appl. Sci. Eng.*, **12**(3):659–661, 2002.
22. R. Miranda, E. Stone, The proto-Lorenz system, *Phys. Lett. A*, **178**:105–113, 1993.
23. S.M. Yu, W.K.S. Tang, J.H. Lü, G.R. Chen, Generation of  $n \times m$ -wing Lorenz-like attractors from a modified Shimizu–Morioka model, *IEEE Trans. Circuits Syst., II, Analog Digit. Signal Process.*, **55**(11):1168–1172, 2008.
24. S.M. Yu, W.K.S. Tang, J.H. Lü, G.R. Chen, Generating  $2n$ -wing attractors from Lorenz-like systems, *Int. J. Circuit Theory Appl.*, **38**(3):243–258, 2010.
25. C.X. Zhang, S.M. Yu, Generation of multi-wing chaotic attractor in fractional order system, *Int. J. Mod. Phys. B*, **44**(10):845–850, 2011.
26. C.X. Zhang, S.M. Yu, Y.Zhang, Design and realization of multi-wing chaotic attractors via switching control, *Int. J. Mod. Phys. B*, **25**(16):2183–2194, 2011.

27. S.M. Yu, J.H. Lü, G.R. Chen, X.H. Yu, Generating grid multiwing chaotic attractors by constructing heteroclinic loops into switching systems, *IEEE Trans. Circuits Syst., II, Analog Digit. Signal Process.*, **58**(5):314–318, 2011.
28. S.M. Yu, J.H. Lü, X.H. Yu, G.R. Chen, Design and implementation of grid multiwing hyperchaotic Lorenz system family via switching control and constructing super-heteroclinic loops, *IEEE Trans. Circuits Syst., I, Fundam. Theory Appl.*, **59**(5):1015–1028, 2012.